World Electric Vehicle Journal

MDPI

Article

Study on the Crashworthiness of a Battery Frame Design for an Electric Vehicle Using FEM

Adrian Daniel Muresanu, Mircea Cristian Dudescu * and David Tica

Department of Mechanical Engineering, Faculty of Automotive, Mechatronics and Mechanical Engineering, Technical University of Cluj-Napoca, 103-105 Muncii Boulevard, 400641 Cluj-Napoca, Romania; adrian.muresanu@campus.utcluj.ro (A.D.M.); tica.ci.david@student.utcluj.ro (D.T.)

* Correspondence: mircea.dudescu@rezi.utcluj.ro; Tel.: +40-264-401663

Abstract: This paper presents an optimized method for evaluating and enhancing the crashworthiness of an electric vehicle (EV) battery frame, leveraging finite element model (FEM) simulations with minimal computational effort. The study begins by utilizing a publicly available LS-DYNA model of a conventional Toyota Camry, simplifying it to include only the structures relevant to a side pole crash scenario. The crash simulations adhere to FMVSS214 and UNR135 standards, while also extending to higher speeds of 45 km/h to evaluate performance under more severe conditions. A dummy frame with virtual mass is integrated into the model to approximate the realistic center of gravity (COG) of an EV and to facilitate visualization. Based on the side pole crash results, critical parameters are extracted to inform the development of load cases for the EV battery. The proposed battery frame, constructed from aluminum, houses a representative volume of battery cells. These cells are defined through a homogenization process derived from individual and pack of cell crash tests. The crashworthiness of the battery frame is assessed by measuring the overall intrusion along the Y-axis and the specific intrusion into the representative volume. This method not only highlights the challenges of adapting conventional vehicle platforms for EVs or for dual compatibility with both conventional and electric powertrains but also provides a framework for developing and testing battery frames independently. By creating relevant load cases derived from full vehicle crash data, this approach enables battery frames to be optimized and evaluated as standalone components, offering a method for efficient and adaptable battery frame development. This approach provides a streamlined yet effective process for optimizing the crash performance of EV battery systems within existing vehicle platforms.

Keywords: Li-ion battery; crashworthiness; electric vehicles; FEM models; dynamic simulation

Citation: Muresanu, A.D.; Dudescu, M.C.; Tica, D. Study on the Crashworthiness of a Battery Frame Design for an Electric Vehicle Using FEM. *World Electr. Veh. J.* **2024**, *15*, 534. https://doi.org/10.3390/wevj15110534

Academic Editor: Qiqi Li

Received: 18 October 2024
Revised: 14 November 2024
Accepted: 18 November 2024
Published: 19 November 2024

1. Introduction

The widespread adoption of lithium-ion (Li-ion) batteries has become a transformative factor in the automotive sector and consumer electronics. Their high energy storage capability, coupled with efficiency and longevity, makes them a popular choice across various industries [1]. Despite their advantages, Li-ion batteries pose significant safety risks, particularly the danger of thermal runaway. This hazardous event can cause the battery to catch fire or explode due to a rapid and uncontrollable increase in temperature, often triggered by physical damage or other failures [2]. Ensuring the crashworthiness of these batteries is essential to mitigate such risks. Crashworthiness is the ability of a battery to endure impact or collision without succumbing to failures like thermal runaway. This is especially critical in electric vehicles, where battery safety directly affects overall vehicle safety [3].

Electric vehicles (EVs) are being seen as a solution for reducing greenhouse gas emissions and lowering reliance on fossil fuels. This trend is bolstered by the substantial environmental advantages they offer and the continuous improvements in battery technology, making EVs more practical and efficient [4]. As the popularity of EVs grows, ensuring

their safety through robust crashworthiness becomes crucial. Crashworthiness is the vehicle's capability to safeguard its occupants during a collision by preserving the structural integrity of the passenger compartment and effectively dissipating crash energy [5]. EVs are equipped with large battery packs that must be adequately protected to prevent hazardous outcomes, such as fires or electric shocks. The structural integrity of the battery enclosure and the vehicle's overall crash management system are critical in mitigating these risks. Several approaches have been investigated to enhance electric vehicle crashworthiness. These include modifying the geometry of the battery frame to increase energy absorption [6–9], optimizing the positioning of the battery within the vehicle structure [10], and developing protective structures along with improved load distribution throughout the body-in-white (BIW) [11,12].

Additionally, regulatory standards like the Federal Motor Vehicle Safety Standard (FMVSS) No. 305 mandate measures to prevent electrolyte spillage and ensure electrical shock protection during and after a crash. This highlights the importance of designing robust battery enclosures and protective structures to prevent hazardous spills and maintain overall vehicle safety [13].

This study introduces a methodology for battery frames design efficiently by reducing reliance on a full vehicle model for simulation. Rather than simulating the entire vehicle in each scenario, we derive critical load parameters from a whole car model crash test with a dummy frame, which mirrors regulations like FMVSS 214 and UNR135. These parameters are then used for targeted battery frame tests at two crash speeds, 32 km/h and 45 km/h, allowing for highly specific analysis without repeatedly running the full vehicle model. This approach is designed to significantly cut computational demands and costs, making it especially useful for battery providers or early design stages—such as when adapting conventional platforms for electric conversion—where access to full vehicle data may be limited.

This methodology focuses on optimizing the battery frame of an EV to minimize intrusion during side pole impacts, ensuring the safety and integrity of the battery pack in a relevant dynamic load case derived from the whole vehicle side pole crash. A simplified vehicle model with a dummy frame will be used to facilitate mass and center of gravity (COG) calculations, focusing on key components and their interactions during a crash. This approach allows for a more manageable and targeted analysis of the critical aspects of crashworthiness. The specific crash scenario studied in this research is the side pole impact, a common and severe type of crash that poses significant risks to the battery pack due to its location and orientation. The optimization process involves balancing the need for minimal intrusion with practical considerations, such as the number of battery cells and overall vehicle weight, as we know these are important EV considerations [14]. Additionally, the study aims to discuss the enhancement of the sill protecting the battery frame, which plays a crucial role in absorbing impact energy and protecting the battery cells [15–18].

The primary objectives of this research are to show a methodology of minimum computational effort to reduce intrusion into the battery compartment during a side pole impact, optimize the structural components for enhanced safety, and ensure compliance with established safety standards. The study will use FEM simulations to analyze the crash performance of the battery frame and its protective aluminum profile, identifying key factors that influence their behavior under impact conditions. The findings will contribute to the development of safer and more reliable electric vehicles, addressing both current challenges and future design considerations.

2. Research of Crash Load Cases Using FEM

The idea of this study is to test different configurations of the battery frame impacting a pole in order to achieve better results in the side pole crash scenarios using LS Dyna software. To set up the load cases for the frame impact as closely as possible to a real scenario, a whole car model was crashed with a dummy frame, from which the necessary parameters for the load case were extracted. The car was subjected to a load case similar to FMVSS 214

or UNR135 regulations, but with two velocities of 32 km/h and 45 km/h, respectively. This approach not only aims to optimize the battery frame but also demonstrates a methodical way to achieve this without having to run the entire car model for every configuration. By obtaining the right load parameters from a specific vehicle and scenario, subsequent tests can focus on the battery frame alone, significantly reducing computational resources and time in battery development.

2.1. Camby Buildup

For this study, the finite element model (FEM) of the 2012 Toyota Camry provided by the Center for Collision Safety and Analysis (CCSA) was selected due to its comprehensive validation and widespread acceptance in crashworthiness research [18,19]. This model offers a highly detailed representation of a midsize sedan, seen in Figure 1, which is critical for accurately simulating and analyzing the impact dynamics involved in crashes. The 2012 Toyota Camry FEM consists of 2,257,280 elements and 2,255,361 nodes, providing a high-resolution mesh that captures intricate vehicle geometries and structural behaviors. The model includes 1086 parts with specific material properties, identified by Part ID (PID), ensuring realistic simulation of different components, such as the body-in-white (BIW), interior structures, and safety systems. The BIW components are modeled with precise details, including over 5000 spot weld points and other connections that replicate the actual manufacturing process. Additionally, the model incorporates comprehensive representations of the vehicle's interior, package, glass, wheels, and other critical elements. Materials are defined using LS-DYNA's extensive material library, incorporating properties like elasticity, plasticity, and some failure criteria tailored for automotive applications.

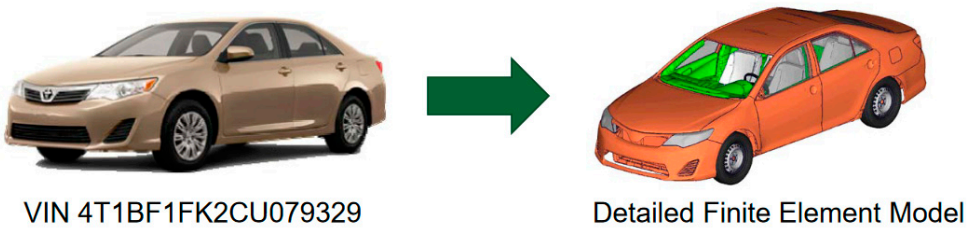

Figure 1. FEM conversion of the sedan Toyota Camry [18].

The choice of this model is predicated on its robustness and detailed documentation, making it a suitable platform for integrating and evaluating the crashworthiness of a lithium-ion electric vehicle (EV) battery under realistic crash scenarios. By using such a detailed and validated model, this study aims to ensure high fidelity in the simulation results, thereby providing reliable insights into the safety performance of the EV battery during side collisions.

To optimize computational resources and focus on the critical aspects of the crashworthiness study, the 2012 Toyota Camry FEM model was simplified. This reduction targeted non-essential components for a pole side crash scenario, retaining only the most relevant structures: the body-in-white (BIW), doors, upper body, and battery frame. The simplification process resulted in a model comprising 1,682,018 elements, 1,676,270 nodes, and 739 parts. This streamlined model configuration allows for a more efficient simulation process, concentrating computational power on the components that directly affect the crashworthiness of the lithium-ion battery frame during a pole side impact.

The simplification procedure, as illustrated in Figure 2, involved the removal of several components. First, the front package was excluded since it does not play a significant role in a pole side impact. Additionally, the powertrain was omitted, focusing the analysis solely on the structural integrity of the vehicle body and the battery frame. The seats and dashboard, which primarily contribute to the interior detail rather than structural response, were also removed. Another significant modification was the exclusion of the fuel tank. As the study involves an electric vehicle (EV) setup, the fuel tank was replaced by a battery

frame to simulate the actual conditions of an EV crash. The back trunk hood was taken out to streamline the model further, ensuring that the computational resources were dedicated to the critical areas under study.

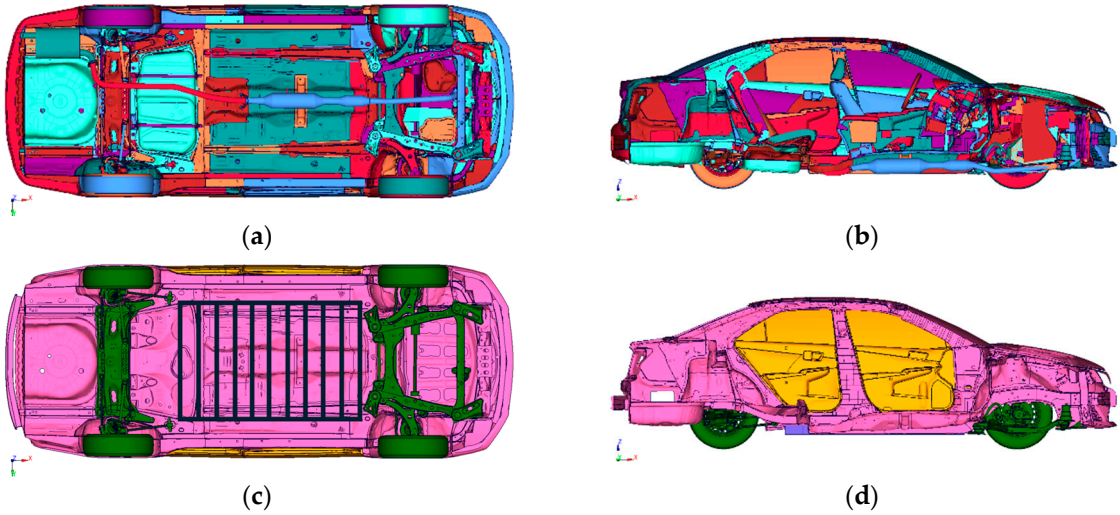

Figure 2. Toyota Camry 2012 FEM simplification: (**a**) original model, bottom view; (**b**) original model, side middle-section view; (**c**) simplified model, bottom view; and (**d**) simplified model, side middle-section view.

Of course, this simplification considerably reduced the mass of the car, necessitating the addition of virtual mass to maintain realistic crash dynamics. To address this, mass was added in three defined part groups located at the front, rear, and middle of the car, as shown in Figure 3, with the help of the LS DYNA entity NSMASS. This function is distributing the total added mass on each of the nodes of the elements belonging to the parts defined in the part groups. The mass distribution was adjusted to achieve 56% at the front and 44% at the rear prior to the addition of the battery frame, resulting in a total vehicle mass of 1480 kg. In total, 650 kg of mass had to be added to compensate for the removed components.

The dummy frame, illustrated in Figure 4, is constructed as a rigid part designed to streamline the simulation process and minimize computational demands. This frame, with dimensions of 1700 mm by 1090 mm and a virtual mass of 300 kg, is fixed to the body-in-white (BIW) in the middle, and it is defined out of contact with the barrier. Its primary function is to alter the vehicle's center of gravity (COG), thereby affecting the impact dynamics and providing a visual reference for barrier intrusion. By adjusting the COG, the dummy frame helps simulate realistic crash conditions. This approach enables the optimization of the battery frame without the need to rerun simulations of the entire car model for each configuration, thereby conserving computational resources and time.

The load case setup of the 2012 Toyota Camry model was aligned with the FMVSS 214 and UNR135 regulations. FMVSS 214 and UN R135 are critical regulations aimed at enhancing side-impact protection in vehicles. FMVSS 214, implemented by the NHTSA in the United States, includes a dynamic side impact test, where a moving deformable barrier (MDB) strikes the vehicle at 54 km/h, and a pole side-impact test, where the vehicle is propelled sideways into a 254 mm rigid pole at 32 km/h, impacting at a 75-degree angle to simulate real-world conditions. This standard focuses on the structural integrity of the B-pillar, side doors, and side structure, as well as the effectiveness of occupant-protection systems. Similarly, UN R135, under UNECE, mandates a pole side impact test at 32 km/h with a 254 mm pole, typically conducted at a 90-degree angle but often considered at 75 degrees for realistic scenarios. Both regulations assess critical components, like the B-pillar, side doors, roof rails, and floor structure, to ensure that vehicles can protect occupants effectively during severe side collisions [20,21].

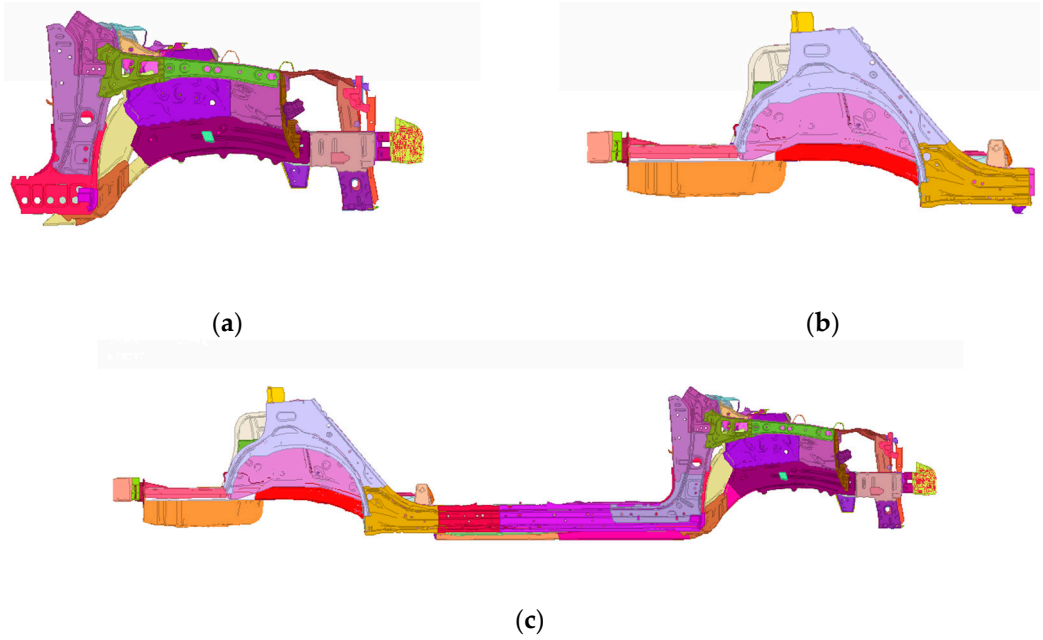

Figure 3. Part groups for virtual mass: (**a**) front-part group, (**b**) back-part group, and (**c**) middle-part group.

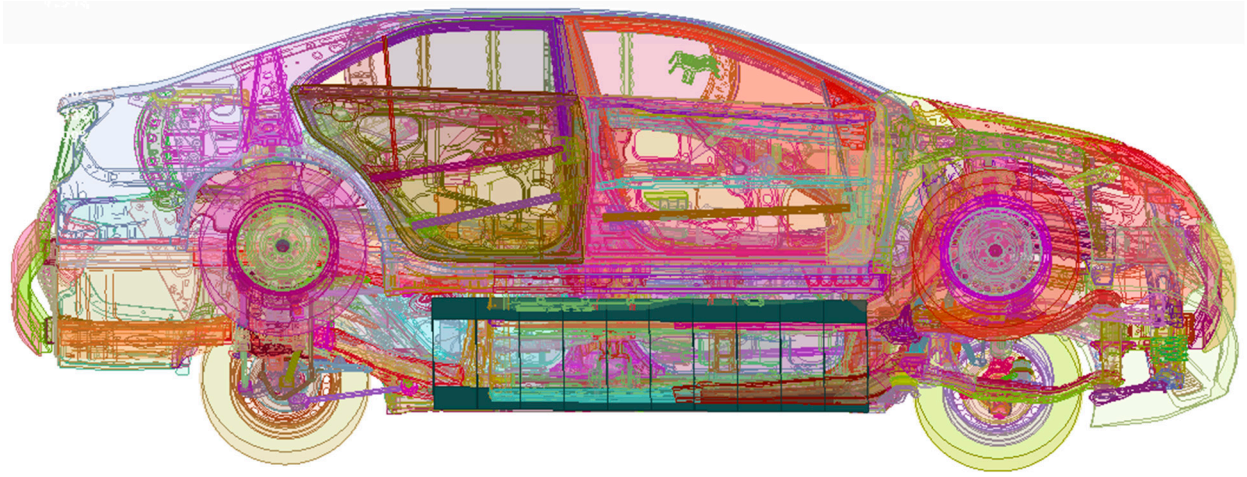

Figure 4. Battery dummy frame under the transparent EV model.

This scenario was chosen, as it represents the worst-case battery intrusion event in a side crash, severely challenging the vehicle's structural integrity, particularly affecting critical components, such as the B-pillar, side doors, sill, and other side structures. Similar to FMVSS 214, the positioning of the pole, diameter of 254 mm, was at 75-degree impact angle with the vehicle moving at 32 km/h and impacting a rigid pole placed where the dummy's head would be located. For robustness, an additional pole position was tested at +200 mm along the vehicle's X-axis (Figure 5), ensuring a comprehensive assessment under varying impact points. Moreover, to explore the limits of crashworthiness, the vehicle was also tested at a higher speed of 45 km/h. This higher-velocity test provides insights into the structural performance of the battery frame under even more extreme conditions. The setup aims to replicate real-world scenarios where the structural integrity of the vehicle and the safety of the occupants are critically evaluated, focusing on the worst-case intrusion and the resultant impact forces on the vehicle's structure.

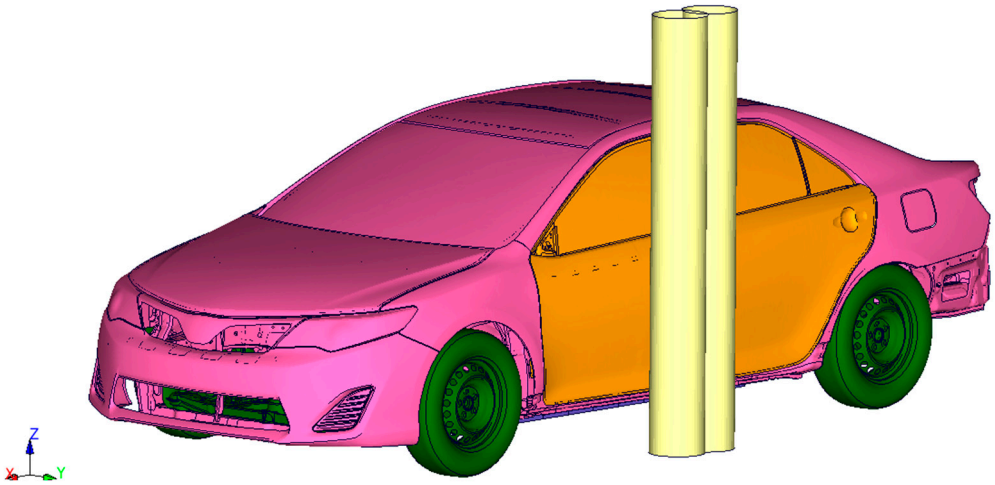

Figure 5. Positions of the pole barriers.

2.2. Frame Load Case Parameters Discussion

Based on the results from the four load cases and the analysis of the internal energy generated during the crash simulation, seen in Table 1, we can establish parameters for the battery frame load cases. Table 1 presents data for four proposed load cases, with each case displaying three columns related to crash energy. The first column shows the total energy of the crash, representing the vehicle's kinetic energy at the moment of impact. The second column lists the total internal energy absorbed by the vehicle throughout the entire crash; this value is lower than the total energy, as some kinetic energy is transferred to vehicle movement around the pole during impact. The third column details the energy absorbed by the vehicle structure up to approximately 0.05 s, when the deformation reaches the battery frame, indicating the structure's initial energy absorption performance before battery compartment intrusion. By drawing an equivalence between the internal energy observed in the car's deformation and the kinetic energy relevant to the battery frame load cases, we can set up the velocity at which the battery frame impacts the pole relatable with the whole vehicle impact. This setup is derived by correlating the energy to the frame's mass, effectively replicating the conditions of a full vehicle crash but within a significantly simplified model. Additionally, by analyzing other factors, such as pole intrusion, we can initiate a discussion regarding the optimal positioning of the battery frame in the Y direction. This includes evaluating the structural behavior and necessary reinforcements for the sill, as well as considering crucial aspects for calculating the crush zone. These considerations are vital for ensuring the integrity and safety of the battery frame under crash conditions.

Table 1. Internal energy parameters from the whole vehicle crash.

Load Case	Total Energy (J)	Internal Energy (J)	Internal Energy +Y Pole Intru. (J)
32 km/h Nominal Pos.	6.81094×10^4	6.08078×10^4	3.8622×10^4
32 km/h +X200 mm Pos.	6.81099×10^4	6.02257×10^4	2.94423×10^4
45 km/h Nominal Pos.	1.33819×10^5	1.20991×10^5	3.64934×10^4
45 km/h +X200 mm Pos.	1.34687×10^5	1.23104×10^5	3.00425×10^4

In a crash scenario, the internal energy of the vehicle or battery structure plays a critical role in determining its behavior upon impact. Internal energy, in this context, refers to the energy absorbed by the vehicle or battery materials and structural components as they deform under crash forces. When a vehicle's structure absorbs a significant amount of energy internally, this absorbed energy limits the force transmitted to the vehicle's occupants or sensitive components, like the battery pack. In engineering simulations, such as those conducted in LS-DYNA, internal energy is a key parameter for assessing the crashworthiness of a design.

The total internal energies for the various load cases are depicted in Figure 6, showing a nearly linear increase in internal energy absorption up to around 0.09 s, after which the vehicle enters a rebound phase, marking the end of structural deformation. The internal energy absorption graph provides insights into the vehicle's dynamic behavior during a pole side crash and how the vehicle's structure responds to the impact, absorbing energy consistently as it deforms.

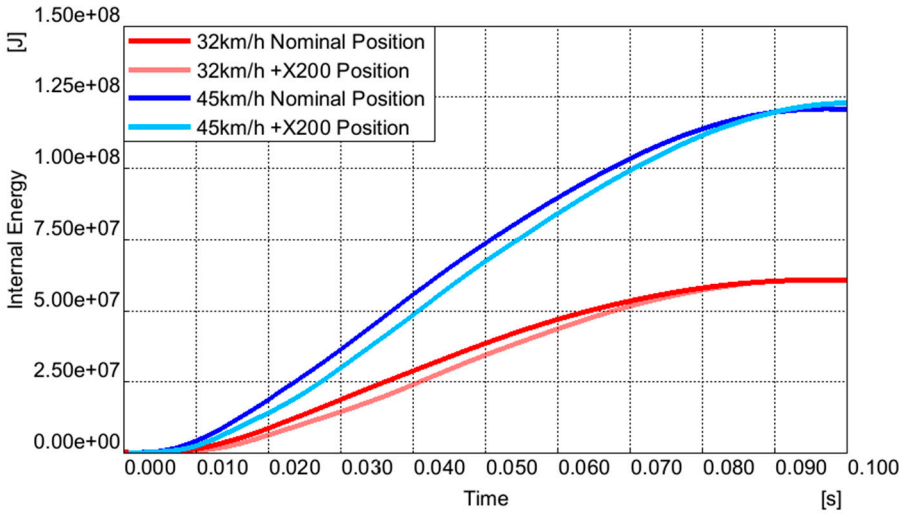

Figure 6. Internal energies graphics of each load case.

A detailed breakdown of the parameters that informed these load cases is presented in Figure 7, offering deeper insight into the factors that influenced the simulation outcomes. This visual and contextual information forms the basis for understanding how internal energy correlates with the behavior of the vehicle and the battery frame during impact, guiding the subsequent analysis and discussion.

The total internal energy absorbed by the vehicle during a crash can be divided into three distinct domains, each defined by the level of pole intrusion into the vehicle's structure and its relation to the position of the battery frame. In a conventional vehicle, the extent of intrusion is primarily governed by ensuring that the biomechanics of the dummies remain within acceptable limits. However, in electric vehicles, this intrusion is more critically constrained by the need to prevent damage to the battery. The battery's vulnerability imposes stricter limitations, making the management of intrusion and energy absorption essential for maintaining both safety and structural integrity.

Considering this, the first domain of energy absorption occurs during the intrusion phase, until the pole makes contact with the battery frame, as seen in Figure 8. In this domain, the total internal energy is absorbed solely by the vehicle's structure and is represented by a green area when the intrusion is not posing any threat to the damage to the battery. This space is crucial for the optimal positioning of the battery frame in the Y direction: the larger the space, the more energy the vehicle structure can absorb before the battery frame is impacted. In this particular case, the pole has to intrude 345 mm until the contact with the battery frame. This energy absorption can be further enhanced by

reinforcing the sill, thereby improving the vehicle's ability to manage crash forces before they reach the battery.

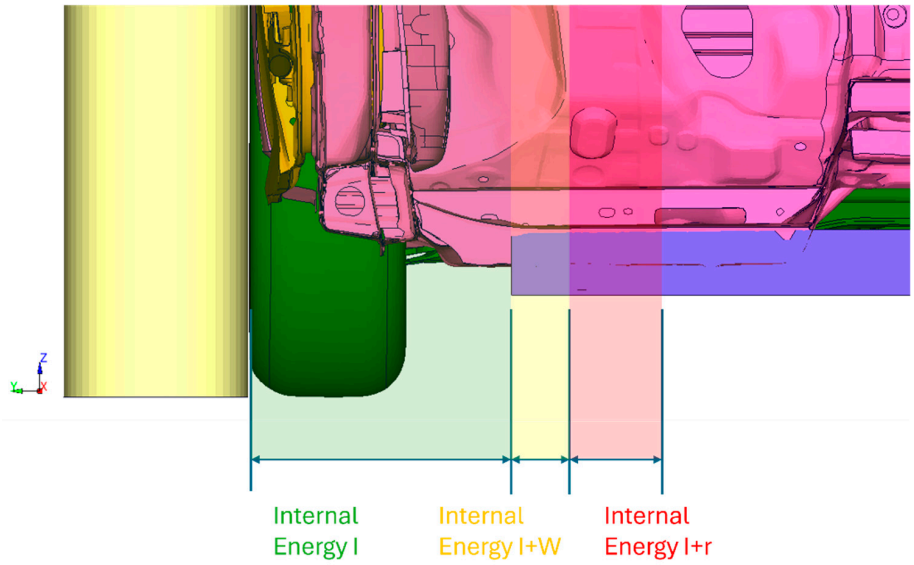

I = Y direction intrusion.
+W = plus the width of the battery profile.
+r = plus the rest of whole crash intrusion.

Figure 7. Energies diagram vs. intrusions.

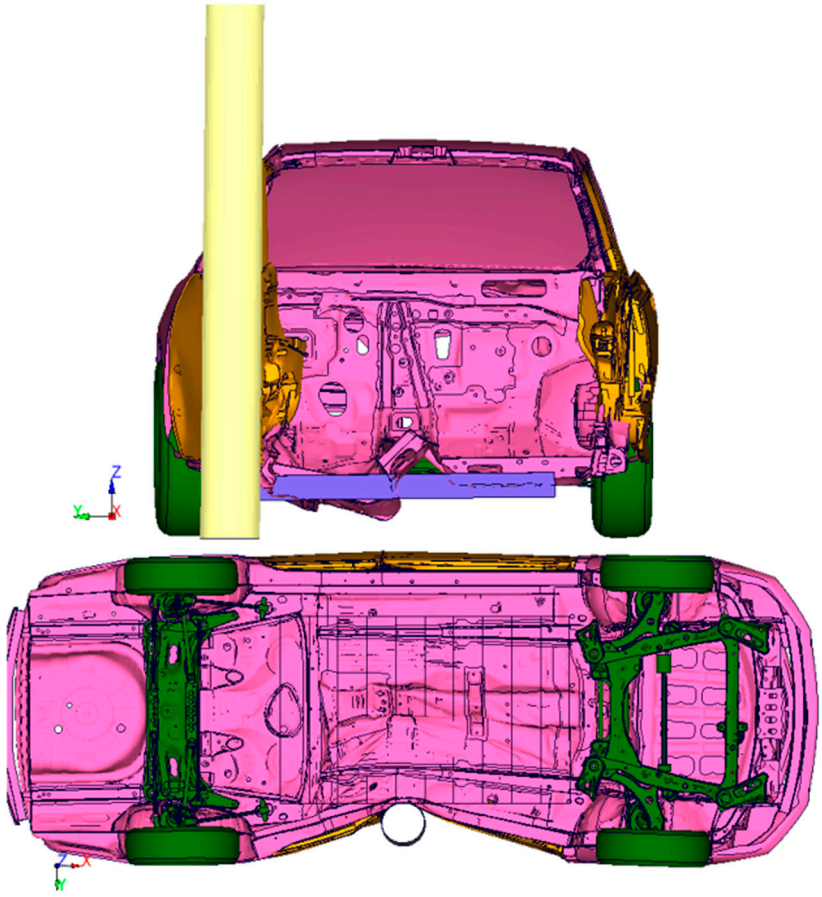

Figure 8. Intrusion of the pole until contact with the battery frame, cut on X and top view.

In the second domain, denoted as I+W, the energy absorption involves both the vehicle structure and the battery frame profile, which has a width of W. This domain is represented by a yellow area and is critical because the deformation of the frame profile plays a key role in halting the intrusion before it can damage the battery modules. In this analysis, the worst-case scenario is considered, where the frame profile is assumed to absorb the entirety of the deformation energy, ensuring maximum protection for the battery. Based on these data, the W of the frame profile can be adjusted to the right value.

The third domain, as illustrated in Figure 9, represents the condition where maximal intrusion occurs in the absence of the battery frame. In this scenario, all internal energy should have already been absorbed by the vehicle structure, as any further intrusion would directly impact the battery modules. Such an event would lead to the most severe consequence—a thermal runaway—highlighting the critical importance of effective energy management in the earlier domains.

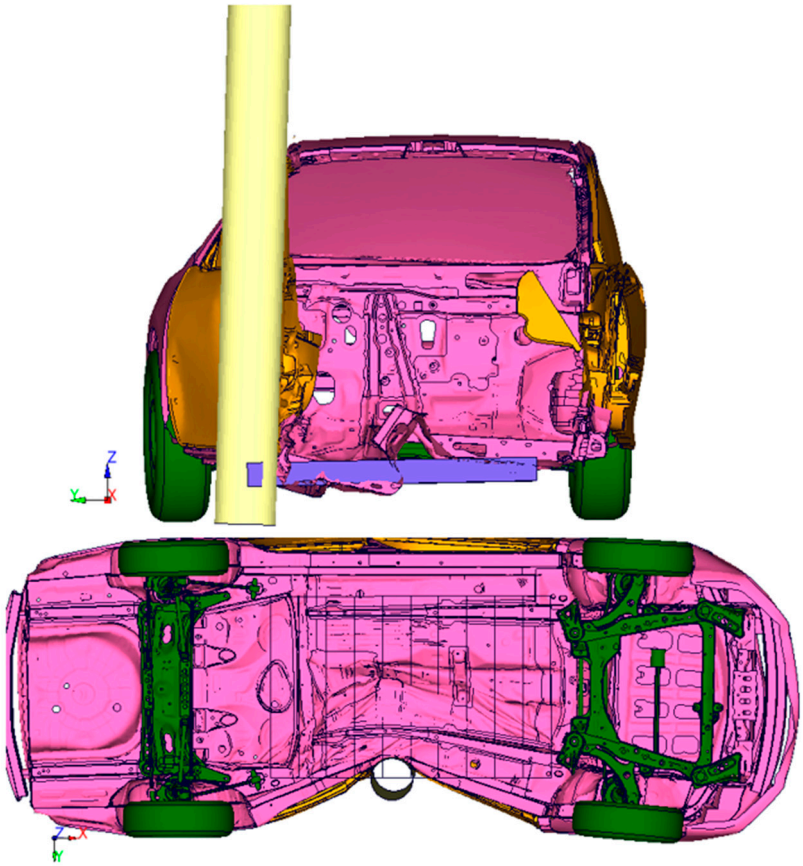

Figure 9. Maximal intrusion of the pole, cut on X and top view.

For the frame load case calculations, the worst-case scenario is assumed by subtracting the energy absorbed in the first domain from the total internal energy. This would mean that the whole internal energy consumed by the structure, after the contact with the frame, is now absorbed by the battery frame. This approach ensures that the remaining energy is considered for the frame load case, emphasizing the need for robust protection in the second domain, which would be the frame profile. Table 2 presents the kinetic energy calculated for each frame load case, along with the corresponding velocities required for a frame with a mass of 300 kg. These data are crucial for understanding the energy dynamics involved and ensuring that the frame is adequately designed to withstand such forces.

Table 2. Kinetic energy and velocity resulted in battery frame load cases.

Load Case	Kinetic Energy (J)	Battery Frame Velocity (km/h)
32 km/h Nominal Pos.	2.21858×10^4	43.8 km/h
32 km/h +X200 mm Pos.	3.07834×10^4	51.6 km/h
45 km/h Nominal Pos.	8.44176×10^4	85.4 km/h
45 km/h +X200 mm Pos.	9.30615×10^4	89.7 km/h

3. Simulation and Study of the Frame Optimization

The load cases under consideration, for the optimization design of the battery crashworthiness, involve simulating the battery frame impacting a pole at the same position where it would be struck in a full vehicle crash. The speeds were selected to approximate challenging impact conditions based on Table 2: the 50 km/h scenario, which reflects a worst case for the 32 km/h vehicle homologation load case speed, while the higher 87 km/h is an average speed between the two positions of the pole in the 45 km/h vehicle load case. This approach ensures a thorough evaluation of the battery frame's performance under a spectrum of realistic and demanding crash conditions. The frame is tested across four different configurations of aluminum profiles and two distinct pole positions for each configuration, as illustrated in Figure 10. The results of these simulations provide critical insights into how each configuration and pole position affects the frame's ability to absorb energy and protect the battery modules from intrusion and potential damage.

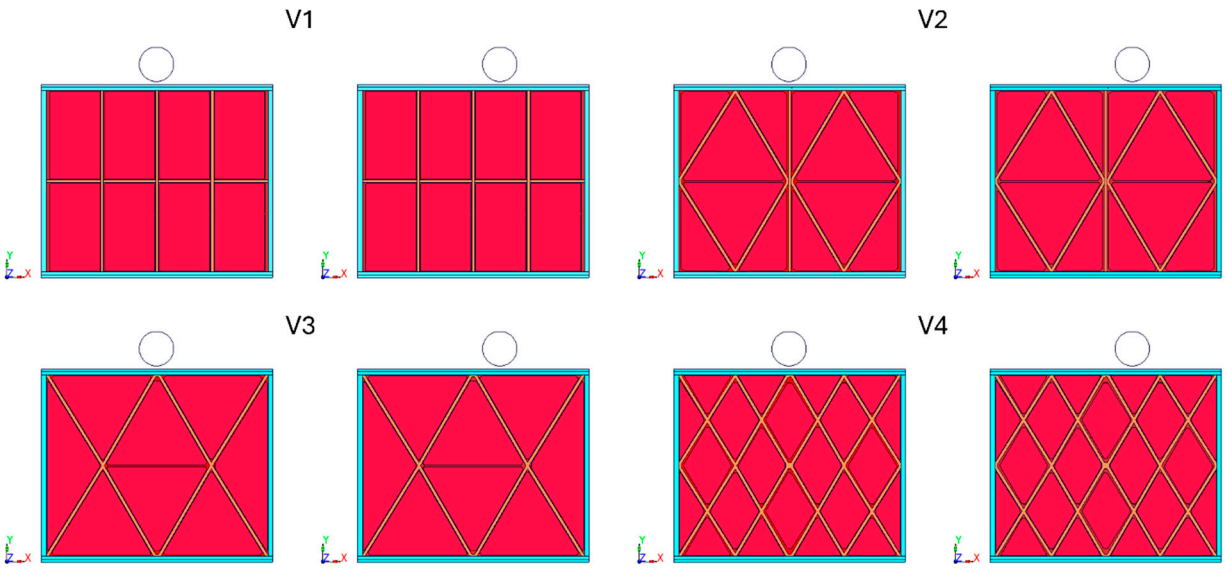

Figure 10. Battery frame configurations.

The model comprises approximately 400,000 elements, varying slightly depending on the configuration. The aluminum profiles are modeled using shell elements, while the interior volume representing the batteries is modeled with solid elements. The average element size is 5 mm, and the simulation time step is set at 0.0005 ms to ensure accuracy and stability in the dynamic analysis. The aluminum profiles are constructed using a basic rectangular profile, which is split in the middle by a transverse surface. The material used is a generic 6061-T6 aluminum, defined as a Type 24 piecewise linear material, with an elastic modulus of 68.9 GPa and a yield strength of 276 MPa. For the battery cells, the

volume is modeled as a homogenized material, representing a pack of cylindrical 18650 Li-ion battery cells. This homogenization assumes that the volume has the same stiffness under compression as a real pack of cells, ensuring that the simulation accurately reflects the mechanical behavior of the battery pack during impact. The placement of the battery cells differs for each configuration due to the different positioning and shapes of the battery packs, with V1 having an area of 1.912528 m^2; V2, 1.833817 m^2; V3, 1.930293 m^2; and V4, 1.726039 m^2.

3.1. Homogenization of the Battery Volume

To homogenize the battery volume, the following method was employed: a pack of nine 18,650 cells was subjected to compression testing, as illustrated in Figure 11.

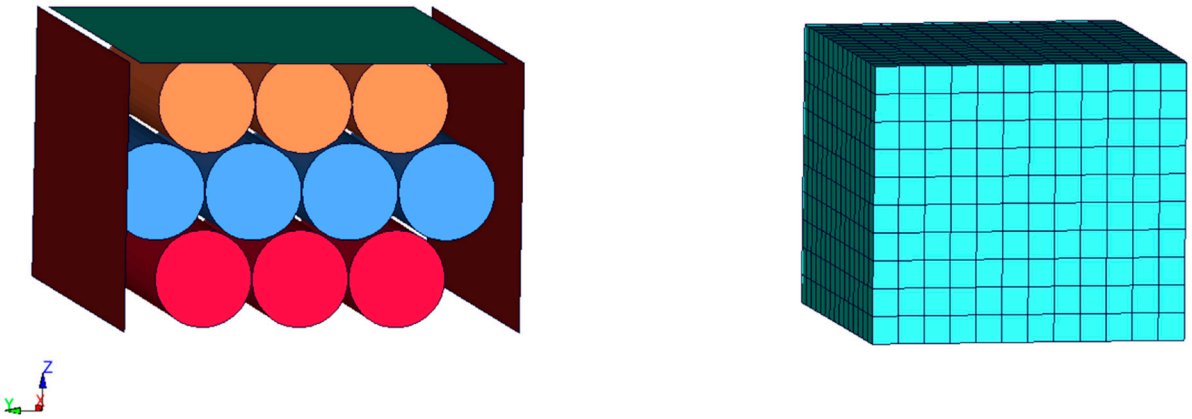

Figure 11. Compression test configuration including 10 cells and representing volume.

The material properties of these cells were previously defined in a prior study [22]. A solid volume representing the cells was created using a Type 24 piecewise linear material model. Instead of using a physical shell press, a load boundary condition was applied during compression to ensure the stability of the simulation in LS-DYNA, as depicted in Figure 11. The material parameters for the solid volume were derived by fitting the load–displacement curve obtained from the compression test of the nine-cell pack.

To validate the scalability of the homogenized material, the volume was doubled in size and subjected to a similar compression test. The goal was to check if the load–displacement curve for the homogenized volume would match the curve obtained from pressing 18 individual cells, as shown in Figure 12.

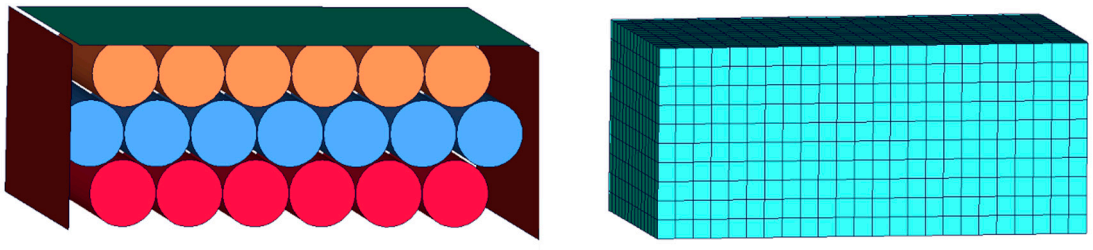

Figure 12. Cell-pressing simulation doubled in size.

The results confirmed that the load–displacement curves for both the smaller and larger packs aligned well, as seen in Figure 13, demonstrating that the homogenization process was successful and that the material model can be reliably scaled for different volumes within the simulation.

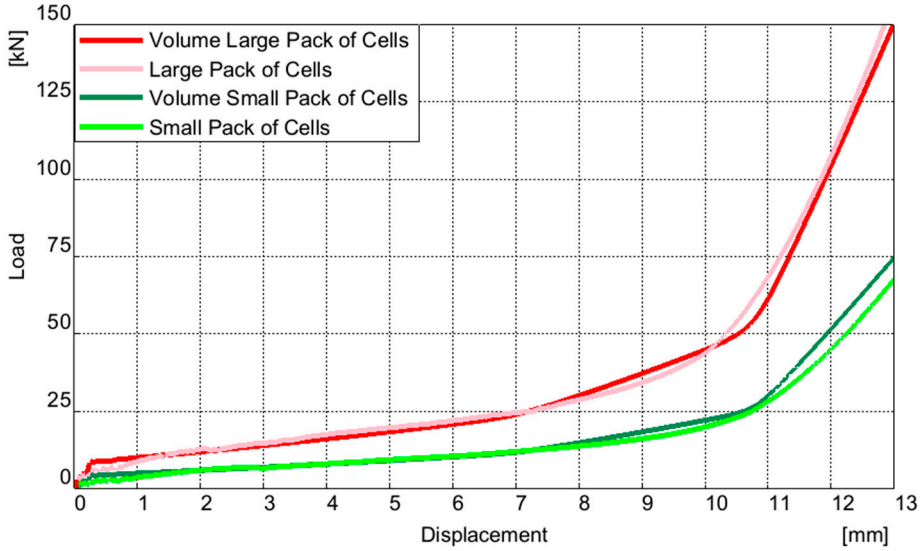

Figure 13. Load–displacement curves matching.

3.2. Results

The results were analyzed with a focus on the overall maximum intrusion of the pole, which is a critical factor that could lead to damage and potentially trigger a thermal runaway in the cells. In addition to assessing the maximum intrusion, the analysis also involved identifying distinct patterns of cell damage for each configuration. This dual approach allowed for a comprehensive evaluation of how different structural setups influence both the extent of intrusion and the specific damage patterns within the battery pack, providing valuable insights for optimizing the safety and integrity of the battery frame under crash conditions.

In the V1 configuration, as shown in Figure 14, the intrusion values for the 50 km/h impact scenario at the nominal position and at +X 200 mm are 86 mm and 89.4 mm, respectively. For the 87 km/h impact scenario, the intrusion values are 173.5 mm and 169.7 mm, respectively. The damage to the cell volume is primarily concentrated in the direction of impact. These results highlight the effect of cell volume densification at higher speeds, where the volume that is impacted the most—at +X 200 mm—exhibits a slightly lower intrusion. This suggests the complexity of interpreting the results, as the densification phenomenon could lead to more localized loading, potentially causing greater damage to the affected cells. While densification may reduce overall intrusion, it also concentrates the forces within a smaller area, increasing the likelihood of severe damage to the cells in that region.

In the V2 configuration, as shown in Figure 15, the intrusion values for the 50 km/h impact scenario at the nominal position and at +X 200 mm are 89.5 mm and 88.1 mm, respectively. For the 87 km/h impact scenario, the intrusion values are 200.5 mm and 174 mm, respectively. The damage to the cell volume is not limited to the impact direction, and it is exacerbated by the collapse of the inner aluminum profiles of the frame. This collapse contributes to additional damage, and with higher intrusions, this configuration is the most vulnerable under severe impact conditions.

In the V3 configuration, as shown in Figure 16, the intrusion values for the 50 km/h impact scenario at the nominal position and at +X 200 mm are 89.7 mm and 107 mm, respectively. For the 87 km/h impact scenario, the intrusion values are 192.5 mm and 202.3 mm, respectively. The damage to the cell volume is primarily concentrated in the direction of impact.

In the V4 configuration, as shown in Figure 17, the intrusion values for the 50 km/h impact scenario at the nominal position and at +X 200 mm are 81.1 mm and 82.8 mm, respectively. For the 87 km/h impact scenario, the intrusion values are 167.9 mm and

167.9 mm, respectively. The damage to the cell volume is primarily concentrated in the direction of impact and symmetric in different positions of the pole. This configuration has the lowest intrusions.

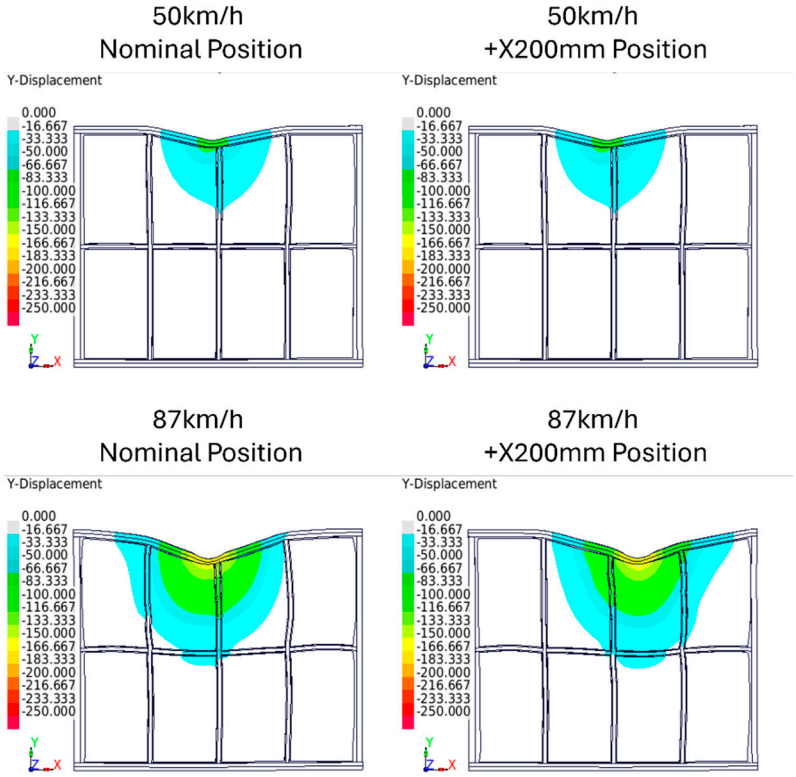

Figure 14. V1 configuration results.

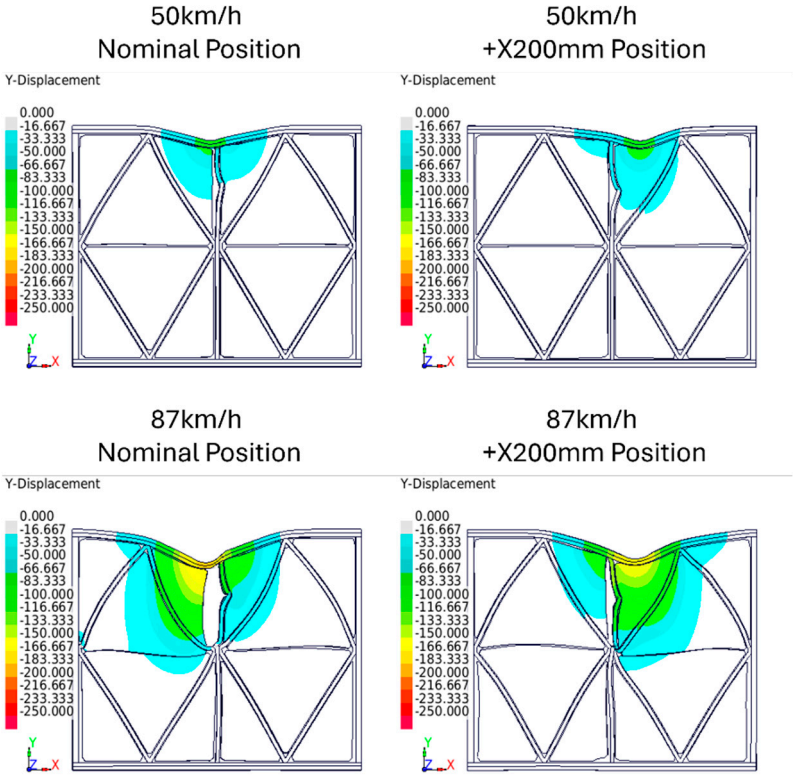

Figure 15. V2 configuration results.

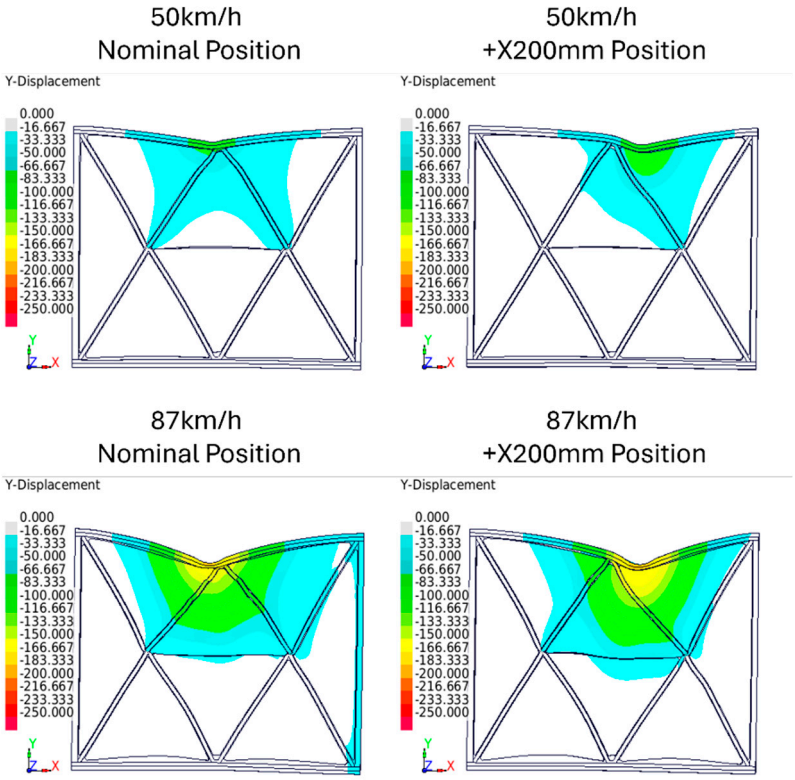

Figure 16. V3 configuration results.

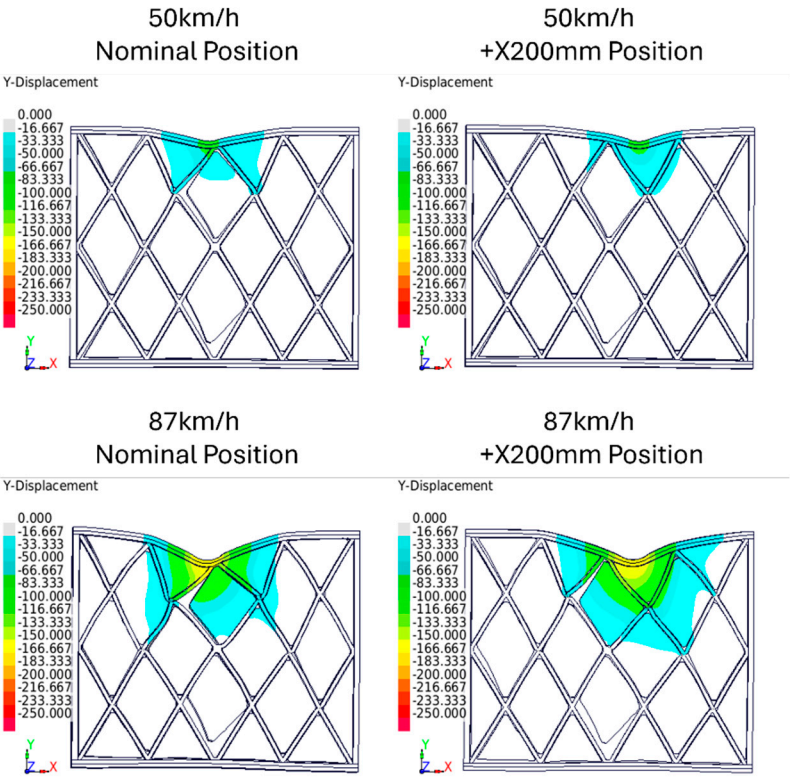

Figure 17. V4 configuration results.

4. Conclusions

In this paper, we developed an optimized method for an EV battery frame design, grounded in the context of a conventional vehicle, with future considerations for platforms

accommodating both conventional and electric vehicles, or battery frame design without full access to the whole vehicle data but with received vehicle crash parameters. We conducted simulations using a simplified model of a Cambry in LS-DYNA, focusing on a side pole crash scenario at two different speeds and two pole positions to ensure robust and reliable results. The model incorporated a dummy battery frame with a virtual mass, which helped approximate the vehicle's central mass more accurately, along with providing a visual representation of the battery's positioning. Using the energy parameters obtained from these simulations, we constructed load cases to optimize the battery frame, examining its performance at impact speeds of 50 km/h and 87 km/h.

In this paper, we also introduced a novel method for defining the material properties of a representative cell pack module. This involved simulating the compression of a pack of nine cells and an equivalent solid volume under a press. From this simulation, a Type 24 material model was developed by fitting the load–displacement curves of the representative volume. To test the reliability of scaling of this material model, we conducted similar simulations with a doubled volume, using the newly defined material. The successful results confirmed the scalability and accuracy of the material model for larger cell volumes.

For the frame design optimization, four load cases were developed, involving impact with a pole at two speeds—50 km/h and 87 km/h—and at two positions: nominal and +X 200 mm. These cases were used to assess which configuration performed best under these conditions. The worst-performing configurations were V2 and V3, which not only exhibited the highest intrusion values but also showed compromised inner structural integrity. The configuration with the lowest intrusion was V4; however, it offered a smaller area for placing the battery cells, with a surface area of 1.726039 m² compared to 1.912528 m² in other configurations. From a crash safety perspective, this study's design optimization of the battery frame under dynamic impact conditions identifies configuration V4, with the lowest intrusion, as the safest option. By minimizing intrusion, V4 reduces the risk of cell damage and potential thermal runway, enhancing overall battery safety in side impacts. This proves that improving the overall stiffness of the battery by design leads to safer electric vehicles.

This methodology offers significant computational advantages by isolating essential crash parameters from a full vehicle model and applying them to a focused battery-only dynamic load case. Unlike traditional approaches, this method eliminates the need for full access to vehicle data, as only key crash parameters are required. This greatly reduces computational demands, as iterative design optimization loops are performed solely on the battery model rather than the entire vehicle, allowing for faster evaluations of various configurations. Additionally, this method is valuable in the pre-design phase of EV development, where benchmarking the battery frame's crashworthiness or other protecting structures, such as the sill, without a finalized vehicle model supports early-stage decision-making and optimization.

Author Contributions: Conceptualization, A.D.M., D.T. and M.C.D.; methodology, A.D.M.; software, A.D.M. and D.T.; validation, A.D.M. and M.C.D.; formal analysis, M.C.D.; investigation, A.D.M., D.T., and M.C.D.; resources, A.D.M., D.T. and M.C.D.; data curation, A.D.M.; writing—original draft preparation, A.D.M.; writing—review and editing, M.C.D.; visualization, A.D.M. and D.T.; supervision, M.C.D. All authors have read and agreed to the published version of the manuscript.

Funding: This research received no external funding.

Institutional Review Board Statement: Not applicable.

Informed Consent Statement: Not applicable.

Data Availability Statement: The data presented in this study are available in this manuscript.

Acknowledgments: The authors express their gratitude to the Technical University of Cluj-Napoca for the financial support of the publication of this article. The authors express their thanks to Arrk R&D Romania for internal HPC usage.

Conflicts of Interest: The authors declare no conflicts of interest.

References

1. Etacheri, V.; Marom, R.; Elazari, R.; Salitra, G.; Aurbach, D. Challenges in the development of advanced Li-ion batteries: A review. *Energy Environ. Sci.* **2011**, *4*, 3243–3262. [CrossRef]
2. Xia, Y.; Li, T.; Ren, F.; Gao, Y.; Wang, H. Failure analysis of pinch–torsion tests as a thermal runaway risk evaluation method of Li-ion cells. *J. Power Sources* **2014**, *265*, 356–362. [CrossRef]
3. Chombo, P.V.; Laoonual, Y. A review of safety strategies of a Li-ion battery. *J. Power Sources* **2020**, *478*, 228649. [CrossRef]
4. Union of Concerned Scientists. (n.d.). The Benefits of Electric Vehicles. Available online: https://www.ucsusa.org/resources/state-benefits-electric-vehicles (accessed on 19 March 2024).
5. Christensen, J.; Wilson, A.; Bastien, C.; Kayvantash, K. Efficient crash structure design for road traffic accidents of tomorrow. *Int. J. Crashworthiness* **2023**, *28*, 629–648. [CrossRef]
6. Haris, A.; Lee, H.P. Vibration, shock and impact analyses of a structural honeycomb battery pack. *Int. J. Crashworthiness* **2023**, *28*, 552–559. [CrossRef]
7. RoUerlich, R.; Ambikakumari Sanalkumar, K.; Bokelmann, T.; Vietor, T. Finite element analysis considering packaging efficiency of innovative battery pack designs. *Int. J. Crashworthiness* **2020**, *25*, 664–679. [CrossRef]
8. Zhang, J.; Ning, L.; Hao, Y.; Sang, T. Topology optimization for crashworthiness and structural design of a battery electric vehicle. *Int. J. Crashworthiness* **2021**, *26*, 651–660. [CrossRef]
9. Shui, L.; Chen, F.; Garg, A.; Peng, X.; Bao, N.; Zhang, J. Design optimization of battery pack enclosure for electric vehicle. *Struct. Multidiscip. Optim.* **2018**, *58*, 331–347. [CrossRef]
10. Kuchenbuch, K.; Vietor, T.; Stieg, J. Optimisation algorithms for the design of electric cars. *ATZ Worldw. eMagazine* **2011**, *113*, 16–19. [CrossRef]
11. Navale, A.B.; Chippa, S.P.; Chougule, D.A.; Raut, P.M. Crashworthiness aspects of electric vehicle design. *Int. J. Crashworthiness* **2021**, *26*, 368–387. [CrossRef]
12. Li, Z.; Duan, L.B.; Cheng, A.G.; Yao, Z.P.; Chen, T.; Yao, W. Lightweight and crashworthiness design of an electric vehicle using a six-sigma robust design optimization method. *Eng. Optim.* **2019**, *51*, 1393–1411. [CrossRef]
13. FMVSS 305; NHTSA. "NATIONAL HIGHWAY TRAFFIC SAFETY ADMINISTRATION LABORATORY TEST PROCEDURE FOR FMVSS 305, ELECTRIC POWERED VEHICLES: ELECTROLYTE SPILLAGE AND ELECTRICAL SHOCK PROTECTION". 2022. Available online: https://www.nhtsa.gov/sites/nhtsa.gov/files/2022-05/Test-Procedure-305-02-February-2022-tag.pdf (accessed on 19 March 2024).
14. Funcke, M.; Schäfer, S.; Sturk, D.; Dufaut, D. Simulation and active protection of li-ion traction batteries. *ATZ Worldw.* **2015**, *117*, 10–15. [CrossRef]
15. Mortazavi Moghaddam, A.; Kheradpisheh, A.; Asgari, M. An integrated energy absorbing module for battery protection of electric vehicle under lateral pole impact. *Int. J. Crashworthiness* **2022**, *28*, 321–333. [CrossRef]
16. Luís Serra Pereira, J.; Calado Marta, A.; Luís Miguel Ouro Colaço, E.; Szolnoky Ramos Pinto Cunha, F.; Calado Marta, A. Preliminary Design and Analysis of a Chassis Side Beam for Stiffness and Crashworthiness of an Electric Vehicle Aerospace Engineering Examination Committee. 2018. Available online: https://mdo.tecnico.ulisboa.pt/wp-content/uploads/publications_MScThesis_Pereira_2018.pdf (accessed on 19 March 2024).
17. Scurtu, L.I.; Szabo, I.; Gheres, M. Numerical Analysis of Crashworthiness on Electric Vehicle's Battery Case with Auxetic Structure. *Energies* **2023**, *16*, 5849. [CrossRef]
18. Development & Validation of a Finite Element Model for the 2012 Toyota Camry Passenger Sedan. Tech Summary. May 2016. Available online: https://www.ccsa.gmu.edu/wp-content/uploads/2016/06/2012-toyota-camry-tech-summary-v5.pdf (accessed on 19 March 2024).
19. 2012 Toyota Camry Detailed Model v5—Validation. Presentation. Available online: https://www.ccsa.gmu.edu/wp-content/uploads/2016/07/2012-toyota-camry-validation-v5.pdf (accessed on 19 March 2024).
20. *49 C.F.R. § 571.214*; Federal Motor Vehicle Safety Standards; Side Impact Protection (FMVSS 214). National Highway Traffic Safety Administration: Washington, DC, USA, 2011.
21. United Nations Economic Commission for Europe. ECE Regulation No. 135: Uniform Provisions Concerning the Approval of Vehicles with Regard to Their Pole Side Impact Performance. 2015. Available online: https://unece.org/fileadmin/DAM/trans/main/wp29/wp29regs/2015/R135e.pdf (accessed on 19 March 2024).
22. Muresanu, A.D.; Dudescu, M.C. Modelling of a Cylindrical Battery Mechanical Behavior under Compression Load. *Batteries* **2024**, *10*, 353. [CrossRef]